

Atmospheric pressure photoionization mass spectrometry of nucleic bases, ribonucleosides and ribonucleotides

A. Bagag, A. Giuliani¹, O. Laprévôte*

Laboratoire de Spectrométrie de Masse, ICSN-CNRS, Avenue de la Terrasse, 91190 Gif-sur-Yvette, France

Received 19 February 2007; received in revised form 16 March 2007; accepted 16 March 2007

Available online 24 March 2007

Abstract

Almost all the ionization techniques have been employed for the analysis of the bases, nucleosides and nucleotides in mass spectrometry, except atmospheric pressure photoionization (APPI). The latter has attracted these last years a growing interest for the analysis of biological molecules. In this work, we report a comprehensive study of the ionization mechanisms under APPI conditions of the bases, nucleotides and nucleosides. In-source fragmentations have been studied first with the photoionization lamp switched off, i.e., under thermospray conditions. It is shown that, in this mode of operation, fragmentations are minor and the compounds do not suffer from thermal degradation. The fragmentation patterns of these biomolecules have been further monitored under both direct and dopant-assisted photoionization conditions for three different dopant molecules (toluene, anisole and acetone). Some fragmentation channels appeared to be dependent on the nature of the dopant employed and the versatility of the fragments generated under APPI conditions originates from the formation of a variety of precursor ions in the ion source.

© 2007 Elsevier B.V. All rights reserved.

Keywords: Atmospheric pressure photoionization (APPI); Nucleobase; Nucleoside; Nucleotide; Fragmentation mechanism

1. Introduction

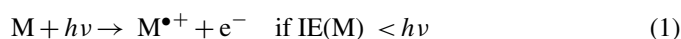
Nucleic acids play a fundamental part in preservation and transfer of the genetic information [1]. The backbone of these molecules is made of alternating sugar (ribose or deoxyribose) and phosphate units bonded together in a long chain, each sugar group being linked to a third type of molecule called a nucleobase.

Some nucleobases have been found in meteorites [2,3] suggesting their possible formation in the interstellar medium [4,5]. The ultraviolet irradiation of the pyrimidine and purine nucleobases is then of the highest interest in view of the possible delivery of these molecules from space to early Earth and of the role that they could have played in the origin and development of life in our planet [6]. The electronic structure and the ionization properties of the nucleic acids are essential for understanding the UV induced degradation pathways of these

important biological molecules. The gas phase reactivity of protonated nucleosides has been investigated by mass spectrometry using mainly their collision-induced dissociation (CID) pathways, which typically begin with the loss of the sugar group leaving the protonated nucleobase. When it further fragments, the latter ion undergoes ring opening and various neutral losses depending on the structure [7,8] of the individual base.

Atmospheric pressure photoionization has attracted in the past few years a growing interest for the analysis of biomolecules. This technique allows almost all kind of solvents to be used, even the most non-polar one, and it is quite insensitive to salts [9].

The ionization mechanism in APPI is based on photoionization of particular species possessing lower ionization energy (IE) than the photon energy ($h\nu$). Usually, a Krypton discharge lamp is used, which produces mostly 10 eV photons. The basic mechanism [10] involves ionization of the analyte (M) according to:



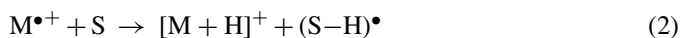
However, the dominant ion observed by APPI is typically $[M+H]^+$, result at variance with usual gas phase photoionization experiments performed in diluted media where the molecular ion

* Corresponding author. Tel.: +33 1 69 82 30 32; fax: +33 1 69 07 72 47.

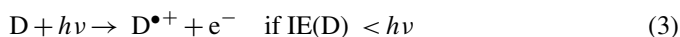
E-mail address: olivier.laprevote@icsn.cnrs-gif.fr (O. Laprévôte).

¹ Present addresses: DISCO Beamline, SOLEIL Synchrotron, BP 48, L'Orme des Merisiers, 91192 Gif-sur-Yvette Cedex, France; Cepia, Institut National de la Recherche Agronomique (INRA), BP 71627, 44316 Nantes Cedex 3, France.

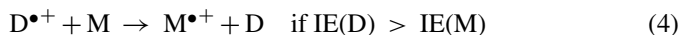
$M^{\bullet+}$ is generally detected [11]. In 2004, Syage [12] solved this apparent discrepancy by showing that the dominant mechanism of $[M+H]^+$ formation by atmospheric pressure photoionization is an hydrogen abstraction reaction by $M^{\bullet+}$ from the protic solvents:



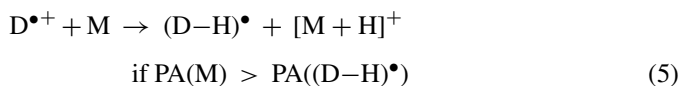
Citing reference [12]: “though the hydrogen abstraction reaction is endothermic in most cases, it is shown that the equilibrium constant is still expected to be much greater than unity in most of the cases studied due to the very slow reverse reaction involving the very low abundant $[M+H]^+$ and $(S-H)^{\bullet}$ species”. However, the direct photoionization of the analyte is not very efficient due to the strong VUV absorption by the nebulizing gases and by the solvent. For this reason, APPI sources may be operated with adjunction of a third molecule, usually referred to as dopant (D), in order to enhance the ionization efficiencies [13,14]. The most widely used compounds are acetone, toluene and anisole. The ionization is initiated by photoionization of the dopant:



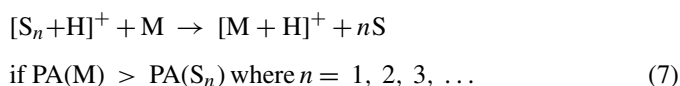
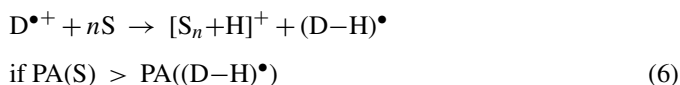
The dopant radical cation $D^{\bullet+}$ may then exchange charge with the analyte if the latter has an ionization energy (IE) lower than that of dopant [13,14]:



This reaction may compete with a proton transfer process if particular conditions on the proton affinities (PA) are fulfilled [13,14]:



The dopant radical cation can also react by proton transfer with solvent clusters if the proton affinity of the cluster is higher than that of the $(D-H)^{\bullet}$ species. The protonated solvent cluster interacting with a molecule of analyte can further lead to the protonated molecule of interest [13,14]:



Therefore, three ionization routes are possible for the positive ionization mode: direct photoionization, charge exchange or proton transfer with the dopant; all reactions depending on the ionization energies and proton affinities of the analyte, solvent and dopant. In the case of dopant-assisted APPI (DA-APPI), considering the relative amount of the dopant with respect to the analyte, it is assumed that photoabsorption of the analyte molecule is very unlikely. We therefore consider that, under such conditions, the ionization mechanisms are entirely ascribed to

those involving the dopant as described at Eqs. (3)–(7) and that the direct photoionization (Eq. (1)) is negligible.

Hitherto less effort has been devoted to the study of the fundamental processes occurring in the APPI source despite their complexity and fundamental interest. In this work, we first have paid attention to the behaviour of the molecules with the photoionization lamp switched off, namely under thermospray conditions. The comparison of the mass spectra obtained by that way to those recorded with the UV lamp switched on allowed us to decipher the consequences of the direct light absorption by the molecules. Addition of a dopant, in order to achieve dopant-assisted APPI experiments, led us to reveal the specific fragmentations controlled by the analyte/dopant interactions.

2. Experimental

2.1. Chemical and compounds

All solvents were HPLC grade. Methanol and acetone were purchased from Prolabo (Fontenay-sous-Bois, France). Water used was bidistilled and filtered on Millipore cartridges (18 M Ω). Toluene 99.5% from SDS (Peypin, France), anisole 99% from Acros Organics (Geel, Belgium) and acetone were used as dopants and introduced at various flow rates using a Harvard syringe pump model 22 (Harvard, Holliston, MA, USA).

Nucleic bases have been provided graciously by Dr. Pascale Clivio (FRE CNRS 2715, Reims, France) and the nucleosides and nucleotides were purchased from Acros Organics (Geel, Belgium).

2.2. Mass spectrometry

The photoionization experiments were carried out by using the PhotosprayTM source (Applied Biosystems, Foster City, CA, USA). This source was fitted with a Krypton PKS 106 lamp (Cathodeon, Cambridge, UK) that generates a continuous flow of mainly 10 eV photons with a minor contribution of 10.6 eV photons. Mass spectra were recorded using a hybrid quadrupole-time-of-flight mass spectrometer (Qstar Pulsar-i, Applied Biosystems). Stock solutions of compounds were prepared in water at a concentration of 10⁻⁴ mol L⁻¹.

The samples were injected by the flow-injection analysis (FIA) method: 20 μ L of the sample solutions were loaded into an injection loop and next eluted with water (called “LC solvent” in the following in analogy with liquid chromatographic separations). The LC solvent was introduced into the photospray ionization source using a HPLC pump Agilent 1100 series (Agilent Technologies, Palo alto, CA, USA) at a flow rate of 200 μ L min⁻¹. The nebulizer gas was dry and clean air.

Mass spectrometric instrumental parameters were adjusted in order to attain the best signal-to-noise ratio and to minimize possible in source collision-induced dissociation (CID). Operating parameters for the nucleic bases were: Ion source voltage (ISV) = 1200 V, declustering potential 1 (DP₁) = 20 V, focusing potential (FP) = 100 V, declustering potential 2 (DP₂) = 15 V. For the nucleosides and nucleotides, the typical parameters were the same except for the ISV value which was adjusted to 1800 V. The

gas flow protecting the lamp was fixed to 2 L min^{-1} . Data were acquired using the Analyst QS software (Applied Biosystems).

3. Results and discussion

3.1. Purine and pyrimidine bases

The mass spectra of the nucleic bases recorded at 400°C with the lamp switched off show the intense ion peaks assigned to $[\text{M}+\text{H}]^+$ ions and sodium cationized species ($[\text{M}+\text{Na}]^+$) for all the studied bases (adenine, thymine, uracil, guanine, cytosine) (spectra not shown). The cationized species observed under such conditions are transferred into the gas phase by a thermospray-like process, that is desolvation of charged species performed in solution, as shown in previous works [15,16]. The thermal degradations of nucleobases and the *in-situ* collision-induced dissociations of their corresponding ions appear to be minor.

Table 1 lists some data concerning the nucleobases which are relevant for the present study. Since the NIST [17] does not recommend any precise value for the ionization energies of the nucleobases, Table 1 reports the minimum and maximum values. From those ionization energy data, it is expected that all the nucleobases may be ionized under APPI conditions, since their ionization energies are all lower than the energy of the photons delivered by the lamp. Hence, switching the lamp on has large consequences on the mass spectra of the bases. The total ion current increases and the absolute ion intensities are significantly more important than in thermospray. Fig. 1 compares the APPI mass spectrum recorded in water for the uracil (Fig. 1a) to that of guanine (Fig. 1b). The mass spectra show the formation of intense $[\text{M}+\text{H}]^+$ ion peaks for all the bases, which is at variance with usual gas phase photoionization experiments performed in diluted media [18], as mentioned previously. Moreover, only intact protonated or cationized molecules are detected without any significant fragment. In the case of uracil, this observation is in agreement with previous photoionization experiments carried out on the isolated (gas phase) molecule, for which the lowest

Table 1
Ionization energies (IE) and proton affinities (PA) of the nucleobases and dopant molecules

Compounds	IE (eV)	PA (kJ mol ⁻¹)
Guanine	7.8–8.2	959.5
Adenine	8.3–8.9	942.8
Cytosine	8.4–9.0	949.9
Thymine	9.0–9.4	880.9
Uracil	9.2–9.8	872.7
Adenosine		989.3
Cytidine		982.5
Uridine		947.6
Toluene	8.83	
Benzyl radical		831.4
Anisole	8.20	
Methoxyphenyl radical		~880
Acetone	9.69	
2-oxo-Propyl radical		820

The data are extracted from the NIST database¹⁷ except for the proton affinity of the methoxyphenyl radical which has been found in reference [19].

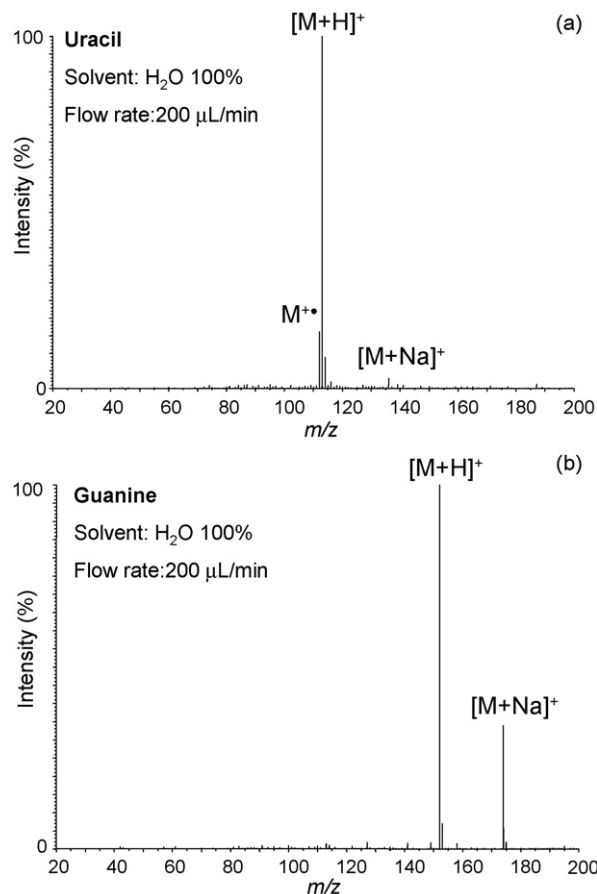


Fig. 1. APPI mass spectra of (a) uracil and (b) guanine, recorded in H_2O at 400°C .

appearance energy for fragmentation was found at 10.95 eV [18]. With regard to the other bases, uracil exhibits a conspicuous behaviour since its molecular radical cation $\text{M}^{\bullet+}$ is detected. The major H-atom transfer reaction must then be considered as competitive to the processes leading to the molecular ions (direct photoionization or charge exchange reaction).

According to Syage [12], the enthalpy of the H-atom transfer reaction (Eq. (2)) can be expressed as:

$$\Delta H = \text{IE}(\text{H}) - \text{IE}(\text{M}) - \text{PA}(\text{M}) + D_{\text{H}}(\text{S}) \quad (8)$$

where $\text{IE}(\text{H})$ and $\text{IE}(\text{M})$ are the respective ionization energies of the hydrogen atom and of the analyte, $\text{PA}(\text{M})$ is the proton affinity of the analyte and $D_{\text{H}}(\text{S})$ is the H-atom bond dissociation energy in the solvent molecule. With $\text{IE}(\text{H}) = 13.6 \text{ eV}$, $D_{\text{H}}(\text{H}_2\text{O}) = 5.16 \text{ eV}$ and $D_{\text{H}}(\text{MeOH}) = 4.08 \text{ eV}$, the reaction enthalpies have been calculated for water and methanol taking into account the minimal value of the ionization potential energy. The results, listed in Table 2, are compared to the $\text{M}^{\bullet+}/[\text{M}+\text{H}]^+$ ratios calculated in both solvent from the mass spectrometry data. According to the obtained reaction enthalpy values, it appears that the H-atom transfer reaction is always endothermic in water, but it is exothermic in methanol for three bases: guanine, cytosine and adenine.

From the intensity ratio given in Table 2, it is seen that for every nucleobases the radical cation is a minor species in both

Table 2
Calculation of the reaction enthalpy values for the H-atom abstraction reaction (Eq. (8)) for the minimal value of IE in Table 1 and intensity ratios of the molecular radical cation to the protonated molecule for each nucleic base in water and methanol

Bases	$\Delta H_{\text{H}_2\text{O}}$ (kJ mol ⁻¹)	ΔH_{MeOH} (kJ mol ⁻¹)	$[\text{M}^{\bullet+}]/[\text{M}+\text{H}]^+$ in H ₂ O	$[\text{M}^{\bullet+}]/[\text{M}+\text{H}]^+$ in MeOH
Guanine	96.3	-7.7	0.01	0.01
Adenine	64.5	-39.5	2.4×10^{-3}	0
Cytosine	48.2	-55.8	2.1×10^{-4}	6.7×10^{-5}
Thymine	279.3	175.3	1.2×10^{-3}	3.45×10^{-3}
Uracil	265.8	161.8	0.16	16.6

solvent, except for uracil. Hence, no trend may be derived within the series of molecules from the comparison of the calculated enthalpies and the intensity ratios. Such a disagreement between the observations and the calculation of the enthalpy in water has been pointed out previously [12]. Although the solvents used in this work were of the highest available purity, ionization of an impurity and subsequent proton transfer to the bases is mentioned for completeness.

The use of dopant-assisted ionization conditions provides additional information on the ionization processes occurring in the APPI source. Fig. 2 displays the mass spectra of uracil (Fig. 2a) and guanine (Fig. 2b) in presence of anisole (at a 0.5 $\mu\text{L min}^{-1}$ flow rate). In this case, the situation is completely reversed with regard to the previous experiment: the molecular

ion $\text{M}^{\bullet+}$ gives a very strong signal with guanine whereas uracil is detected only in its protonated form. The mass spectra of the other nucleobases are similar to that of uracil (Fig. 2a), without any molecular ion or other fragment ion. From Table 1, it appears that the proton affinities of the $[\text{D}-\text{H}]^{\bullet}$ species formed from the dopants are lower than those of the nucleobases, thereby justifying their facile protonation under DA-APPI conditions (Eq. (5)). The case of the guanine molecule is particularly interesting inasmuch as it presents the highest proton affinity (which should be in favor of protonation reactions, Eq. (5)) and the lowest ionization energy (which could induce efficient charge transfer reactions, Eq. (4)). It is worth noting that guanine is the only compound for which the ionization energy is lower than that of anisole (Table 1). In agreement with the respective ionization energies of guanine and anisole, the charge transfer reaction (Eq. (4)) clearly takes place with this dopant as shown in spectrum 2b. This condition is not fulfilled for the other nucleobases. This result helps to understand the origin of the radical cation which is observed in the case of uracil in the absence of dopant. The comparison of the mass spectra of this compound shown in Figs. 1 and 2a clearly demonstrates that the radical cation was formed by photoabsorption (Fig. 1a, Eq. (1)), a process which can not be observed when a dopant is introduced in the source and undergoes the photoionization reaction in place of the analyte. All these observations confirm our assertion that direct photoionization of the analyte may be neglected under dopant-assisted APPI. Depending on the relative proton affinities and ionization energies of the dopant and analyte molecules, their interaction leads to charge exchange reaction or H-atom transfers, or both.

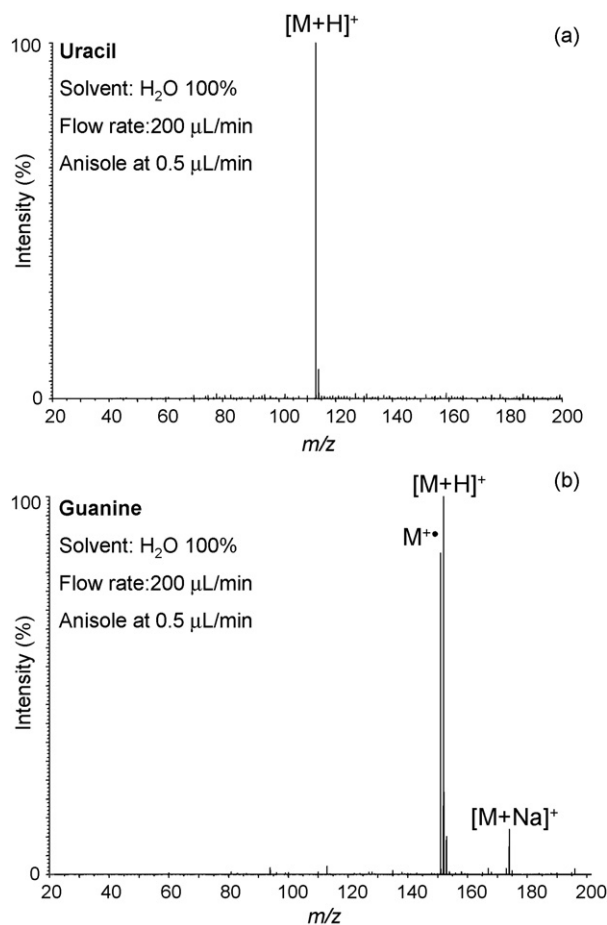
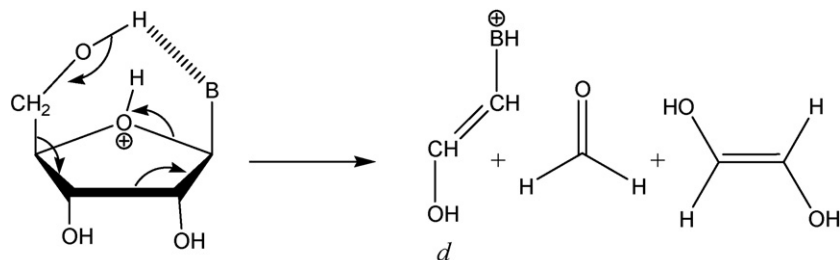


Fig. 2. Dopant-assisted APPI mass spectra recorded at 400 °C of (a) uracil and (b) guanine with infusion of anisole.

3.2. Ribonucleosides

The APPI mass spectra of the ribonucleosides (adenosine, cytidine, uridine and guanosine) are very similar to those acquired under thermospray conditions (i.e., with the lamp switched off) but the total ion current is much higher with the lamp on. The Fig. 3a displays the photoionization mass spectrum of uridine recorded at 500 °C in water. The major peaks correspond to the cationized species $[\text{M}+\text{Na}]^+$ and $[\text{M}+2\text{Na}-\text{H}]^+$ together with a fragment assigned to the protonated nucleobase, which arises from the loss of the neutral sugar moiety [20,21].

Introduction of the dopant has significant consequences on the mass spectra of the ribonucleosides. As exemplified by Fig. 3b, infusion of toluene at 5 $\mu\text{L min}^{-1}$ in the ion source reduces strongly the $[\text{M}+\text{Na}]^+$ ion peak with respect to that of the $[\text{M}+\text{H}]^+$ ion. The loss of the ribose moiety leading the protonated



Scheme 1.

base (BH_2^+ , base peak) is still observed without any other fragmentation process.

Changing toluene by acetone as the dopant induces some modifications of the DA-APPI mass spectrum of uridine (Fig. 3c). Beside the protonated molecule and the BH_2^+ ion peaks, additional fragment ions show up at m/z 227 ($[\text{M}+\text{H}-\text{H}_2\text{O}]^+$) and m/z 155. The latter one corresponds to a *d* ion according to the nomenclature proposed by McCloskey et al. [22,23] (Scheme 1). For uridine, it appears only when acetone is used as a dopant and its relative intensity increases when the acetone flow rate rises. The formation of this *d* ion should thus

be related to the difference between acetone and toluene with regards to the protonation reaction of the analyte. The lowest proton affinity of the 2-oxo-propyl radical (which corresponds to the $[\text{D}-\text{H}]^\bullet$ species formed from acetone) could increase the protonation rate of the nucleoside on the less basic sugar part of the molecule thus inducing the fragmentation reaction shown in Scheme 1. According to Wilson and McCloskey [22], the proton affinity of the sugar moiety is below 865 kJ mol^{-1} . Since the *d* fragment is not observed using toluene for uridine (Fig. 3b), the proton affinity of the ribose moiety should stand between those of the benzyl radical ($\text{PA} = 831 \text{ kJ mol}^{-1}$) and of the 2-oxo-propyl radical ($\text{PA} = 820 \text{ kJ mol}^{-1}$). The assumption of a protonation on the sugar moiety of the ribonucleosides as origin of *d* ions is reinforced by the observation of a concomitant water loss (Fig. 3c).

The influence of the dopant properties on the behaviour of the analyte molecule under DA-APPI conditions is further illustrated by the case of adenosine. Fig. 4a displays the mass spectrum of adenosine recorded with $10 \mu\text{L min}^{-1}$ of acetone. The same fragment ions as for uridine (Fig. 3c) are observed but with different relative intensities: the base peak corresponds to the protonated molecule and the relative abundances of the two main fragments $[\text{M}+\text{H}-\text{H}_2\text{O}]^+$ and BH_2^+ are significantly reduced. The higher stability of the $[\text{M}+\text{H}]^+$ ion formed from adenosine is likely to be related to its higher proton affinity with respect to uridine ($989.3 \text{ kJ mol}^{-1}$ versus $947.2 \text{ kJ mol}^{-1}$ for uridine, see Table 1). By using toluene in place of acetone, the $[\text{M}+\text{H}-\text{H}_2\text{O}]^+$ and BH_2^+ ion peaks remain at a similar level but the appearance of a fragment at m/z 164 and of the $\text{M}^{\bullet+}$ ion is particularly noteworthy (Fig. 4b), a phenomenon which could be attributed to the higher PA value of the benzyl radical. The use of anisole confirms this hypothesis. With this dopant, for which the $[\text{D}-\text{H}]^\bullet$ radical possesses the highest proton affinity (Table 1), the protonation of the analyte become a minor process (Fig. 4c). By contrast, other reaction pathways are spectacularly enhanced such as those leading to the *d* fragment and to the one at m/z 164, which was assigned to a *c* fragment ion in the McCloskey's nomenclature [22]. Consequently, the *d* and *c* fragments could originate from an other precursor ion than the protonated molecule. In this context, the appearance of the molecular ion $\text{M}^{\bullet+}$ of adenosine with toluene and its very high abundance with anisole must be taken into account. According to Shaw et al. [23] who reported the formation of *c* and *d* ions under electron impact ionization (Scheme 2), we suggest that these fragments could originate from the radical cation $\text{M}^{\bullet+}$ of adenosine formed by charge transfer with the dopant radical

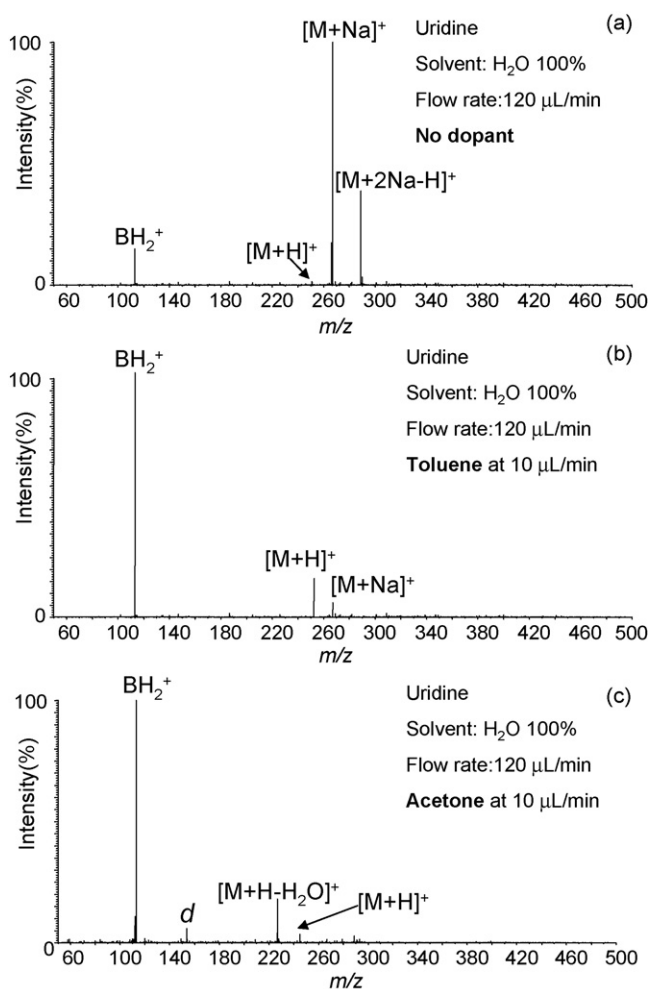
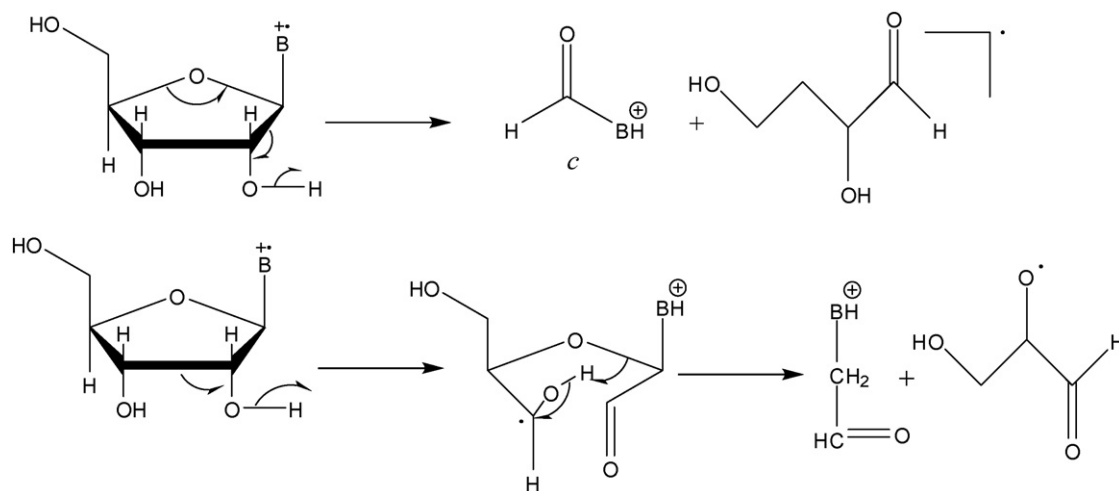


Fig. 3. APPI mass spectra of uridine recorded at 500°C (a) without dopant, (b) assisted with toluene, and (c) with acetone.



Scheme 2.

cation. The comparison of the ionization energies of the three dopants then leads to an apparently paradoxical result: the charge transfer reactions are all the more favourable as the ionization energies of the dopant are low (Table 1). Two different factors have however to be taken into account. First, the charge exchange reaction is competitive to the proton transfer: if the latter reaction rate is lowered, it increases the relative rate of the former. Secondly, as demonstrated in a previous work [24], the photoionization cross section of anisole is approximately two-fold that of toluene, thus increasing the abundance of radical cations able to react with the analyte.

As a consequence, it appears that the *d* fragment ion could originate either from a molecule protonated at the ribose part or from the radical molecular ion.

3.3. Deoxyribonucleosides

Deoxyribonucleosides behave similarly to ribonucleosides with respect to thermospray ionization and direct photoionization. Fig. 5 shows the mass spectrum of deoxyadenosine with $10 \mu\text{L min}^{-1}$ flow rate of toluene. Whatever the dopant used, the mass spectra of the deoxyribonucleosides are dominated by fragment ions originating from successive dehydrations, from

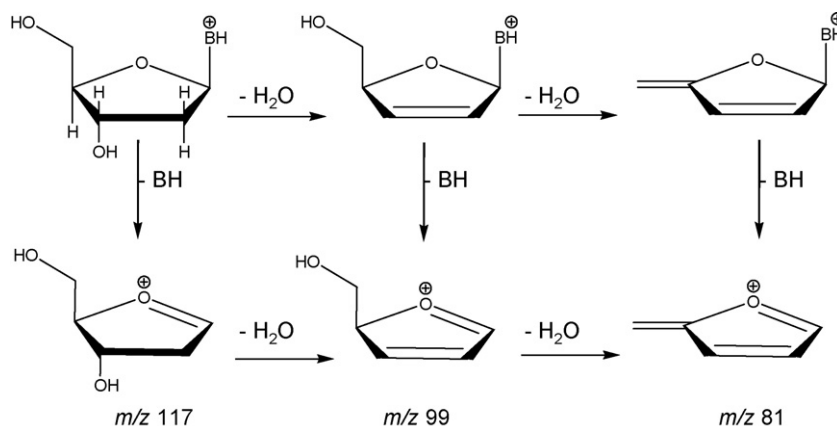
which neutral base losses might occur, as depicted in Scheme 3 [25].

The fragment ions at m/z 117 ($[\text{M}+\text{H}-\text{BH}]^+$) and m/z 81 are observed in Fig. 5, whereas the m/z 99 ion ($[\text{M}+\text{H}-\text{BH}-\text{H}_2\text{O}]^+$) is of too low abundance to be detected. The ions corresponding to the protonated bases are observed for all nucleosides.

In contrast to the ribonucleosides, the water loss that characterizes the presence of the proton on the sugar moiety is not accompanied by the formation of *d* ion. Other processes are observed such as the loss of a second molecule of water or of H_2 from both $[\text{M}+\text{H}]^+$ and $[\text{M}+2\text{Na}-\text{H}]^+$ precursor ions. The absence of *c* ions does not allow us to propose the existence of radical species $\text{M}^{\bullet+}$ which, moreover, are not detected in the spectra.

3.4. Ribonucleotides

Three ribonucleotides, cytidine-5'-monophosphate (CMP), adenosine-5'-monophosphate (AMP) and uridine-5'-monophosphate (UMP) have been studied under thermospray conditions and exhibit analogous behaviours. Fig. 6a displays the thermospray mass spectrum obtained for AMP. For all nucleotides, the thermospray spectra show the formation of



Scheme 3.

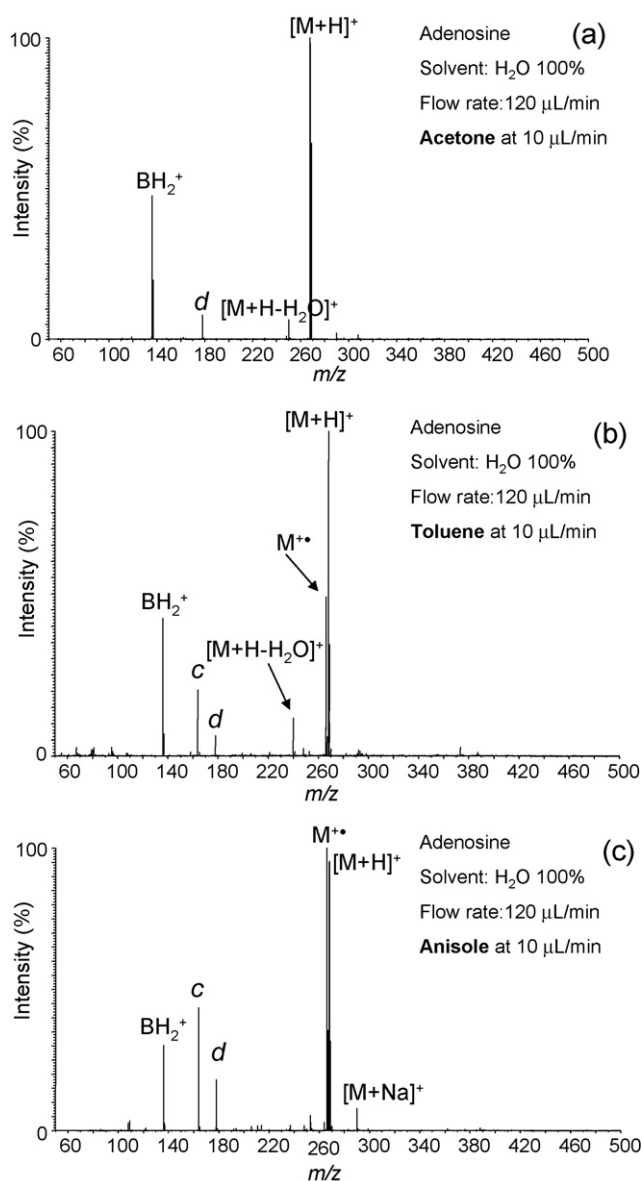


Fig. 4. DA-API mass spectra of adenosine recorded at 500 °C using different dopants: (a) acetone, (b) toluene, and (c) anisole.

mono- and disodiated molecular species along with a less abundant protonated molecule. Fragment ions corresponding to [M+H-HPO₃]⁺ and [M+Na-HPO₃]⁺ are generated from the protonated and sodium-cationized nucleosides, respectively. A consecutive loss of water can also arise from the [M+H-HPO₃]⁺ fragments but not from the cationized ions. Mechanistic studies [25] have reported that, under CID conditions, the formation of the protonated nucleobase (BH₂⁺) involves the assistance of the phosphate group, leading to a very stable cyclic phosphoribose molecule (Scheme 4). The corresponding ion peaks are clearly present in all thermospray spectra as exemplified by that of AMP (Fig. 6a). Under direct photoionization conditions (Fig. 6b), the same fragment ions are detected but with significantly different relative abundances. The contribution of the sodium-cationized ions to the ion current is reduced, thus underlying the increase amount of protonated molecules by photoionization. In addition,

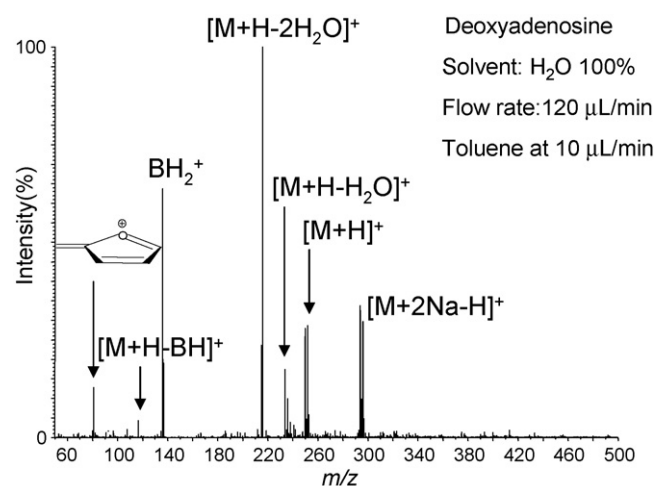


Fig. 5. DA-API mass spectrum of deoxyadenosine recorded at 500 °C using toluene as dopant.

weak *c* and *d* fragment ion peaks are also present. By using acetone as dopant, the DA-API mass spectrum of AMP shows similar features (Fig. 7a). Cationized and protonated molecules are observed along with the BH₂⁺, [M+Na-HPO₃]⁺ and [M+H-HPO₃]⁺ fragment ions, with a further reduced intensity of the

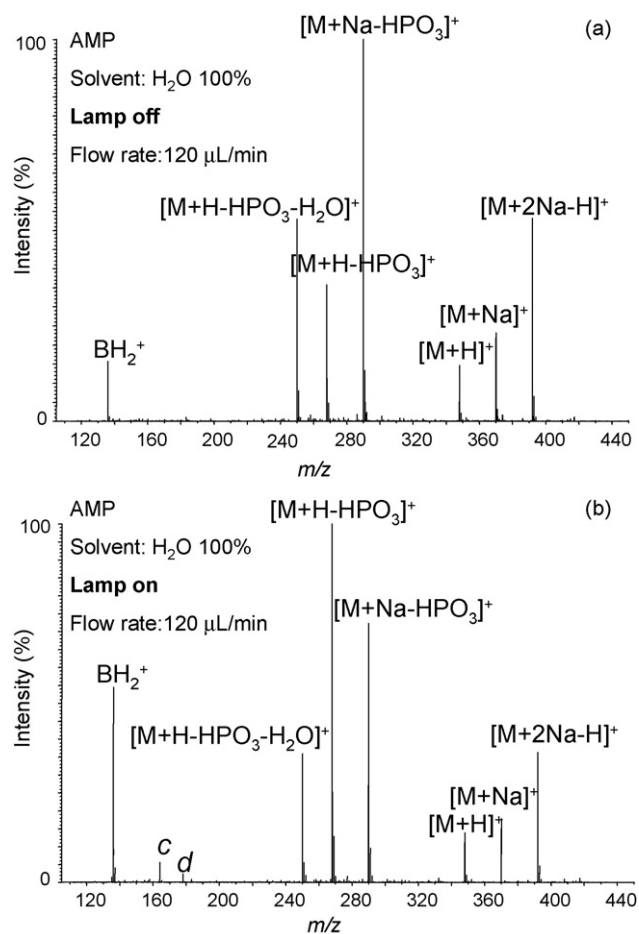
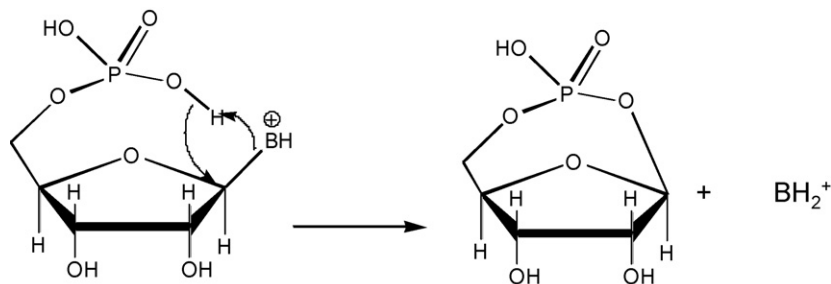


Fig. 6. (a) Thermospray mass spectrum of AMP recorded at 500 °C; (b) APPI mass spectrum of AMP (without dopant) in the same conditions.



Scheme 4.

sodium-containing ions. Similarly to the direct photoionization (Fig. 6b), *c* and *d* fragments of low abundance are observed. Actually, the only difference with the spectrum obtained without dopant is the absence of consecutive loss of water from the $[M+H-HPO_3]^+$ fragment ion.

With regards to AMP, UMP shows a very different behaviour. Fig. 7b shows the DA-APPI mass spectrum of UMP with $10 \mu\text{L min}^{-1}$ of acetone infused. In this case two consecutive losses of water from the $[M+H]^+$ ion are observed, which were absent from the mass spectrum of AMP (Fig. 7a). Moreover, the $[M+H-HPO_3-H_2O]^+$ ions are abundant, at the expense of the $[M+H-HPO_3]^+$ species, in contrast to the AMP molecule.

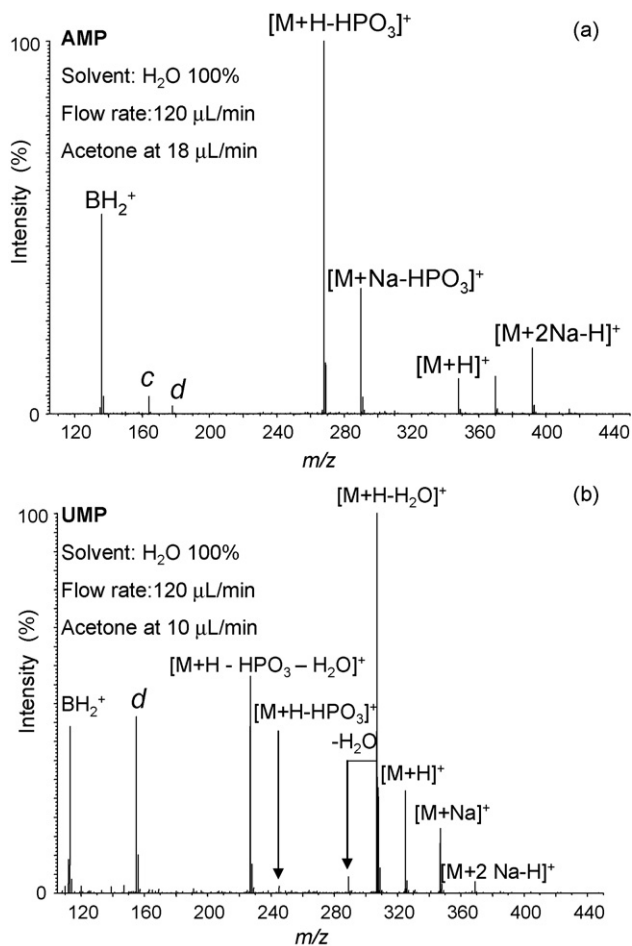


Fig. 7. DA-APPI mass spectra recorded at 500°C of (a) AMP and (b) UMP. Dopant: acetone.

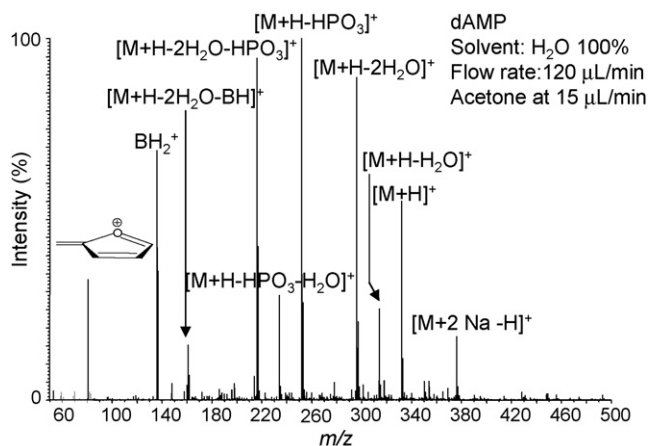


Fig. 8. DA-APPI mass spectrum of dAMP recorded at 500°C using acetone as dopant.

In addition, Fig. 7b exhibits a quite intense *d* fragment ion and no *c* ion. Similarly to the ribonucleoside uridine, these abundant losses of water and the presence of abundant *d* fragment ions suggest an efficient protonation on the ribose moiety of UMP with acetone. The noticeable differences in the fragmentation patterns between protonated UMP and AMP thus underline the pre-eminent role of the protonation sites on their gas phase behaviour. The much higher proton affinity of adenine than that of uracil could enhance significantly the protonation rate of the nucleic base for AMP and of the ribose moiety for UMP. In the case of AMP and in the same way as for the corresponding nucleoside adenosine, minor charge exchange reactions could occur, leading to a weak but significant *c* ion peak.

3.5. Deoxyribonucleotides

The following deoxyribonucleotides have been studied: 2'-deoxyadenosine-5'-monophosphate (dAMP), 2'-deoxycytidine-5'-monophosphate (dCMP), 2'-deoxyguanosine-5'-monophosphate (dGMP) and 2'-deoxythymidine-5'-monophosphate (dTMP). They all exhibit very similar behaviours and therefore only the case of dAMP will be presented. The DA-APPI mass spectrum of dAMP with acetone is displayed at Fig. 8. In correspondence with the case of ribonucleotides (Fig. 7), protonated and sodium-cationized molecules are of low abundance and relatively intense fragment ions are observed. The latter appeared not to be dependant on the nature of the

dopant. The consecutive losses of phosphoric acid, water and nucleic base are more abundant for d(AMP) than for AMP. The same observation was made with nucleosides molecules.

4. Conclusions

This work reports on a comprehensive mass spectrometry study related to nucleobases, nucleotides and nucleosides under APPI conditions. The peculiar features of this ionization technique have been evidenced by direct comparison of the mass spectra with those acquired under thermospray ionization conditions (i.e., with the UV lamp switched off). While fragmentation was little in thermospray, it revealed especially important under dopant-assisted photoionization conditions which show competitive charge transfer and proton transfer reactions. For nucleosides and nucleotides, the *c* ions appear to come from radical species $M^{\bullet+}$. The *d* fragment ions, for their part, can have a double origin: the molecular ions $M^{\bullet+}$ for one hand and, on the other hand, the protonation on the ribose moiety. The protonation rate of the ribose depends strongly on the difference of proton affinities between the bases and the molecules of dopant. The differences in the extent of fragmentation of $[M+H]^+$ ions between the nucleotides and the nucleosides may indicate a real difference in the ease of decomposition of these protonated species, thus showing the importance of the phosphate group. Moreover, successive dehydration reactions occur more easily from deoxyribose containing compounds than from ribose derivatives. In conclusion, the great versatility of fragmentations in APPI comes from the formation of a variety of precursor ions which can be either (radical) molecular ions or molecules protonated at various sites. In that context, the relative ionization energies and proton affinities of the sample and dopant molecules have been shown to play a key role in the relative abundance of these different precursor ions.

References

- [1] C. Périgaud, G. Gosselin, J.-L. Imbach, *Nucleosides Nucleotides* 11 (1992) 903.
- [2] P.G. Stocks, A.W. Schwartz, *Nature* 282 (1979) 709.
- [3] A. Shimoyama, S. Hagishita, K. Harada, *Geochem. J.* 24 (1990) 343.
- [4] S. Chakrabati, S.K. Chakrabati, *Astron. Astrophys.* 354 (2000) L6.
- [5] I.W.M. Smith, D. Talbi, E. Herbst, *Astron. Astrophys.* 369 (2001) 611.
- [6] A. Brack (Ed.), *The Molecular Origins of Life*, Cambridge University Press, Cambridge, UK, 1998.
- [7] J.M. Gregson, J.A. McCloskey, *Int. J. Mass Spectrom. Ion Processes* 165/166 (1997) 475.
- [8] B. Porcelli, L.F. Muraca, B. Frosi, E. Marinello, R. Vernillo, A. De Martio, S. Catinella, P. Traldi, *Rapid Commun. Mass Spectrom.* 11 (1997) 398.
- [9] S.J. Bos, S.M. van Leeuwen, U. Karst, *Anal. Bioanal. Chem.* 384 (2006) 85.
- [10] J.-P. Rauha, H. Vuorela, R. Kostianen, *J. Mass Spectrom.* 36 (2001) 1269.
- [11] J. Berkowitz, *Photoabsorption, Photoionization, Photoelectron Spectroscopy*, Academic Press, New York, 1979, p. 93.
- [12] J.A. Syage, *J. Am. Soc. Mass Spectrom.* 15 (2004) 1521.
- [13] T.J. Kauppila, T. Kotiaho, R. Kostianen, A.P. Bruins, *J. Am. Soc. Mass Spectrom.* 15 (2004) 203.
- [14] T.J. Kauppila, T. Kuuranne, E.C. Meurer, M.N. Eberlin, T. Kotiaho, R. Kostianen, *Anal. Chem.* 74 (2002) 5470.
- [15] S. Cristoni, L.R. Bernardi, I. Binunno, F. Guidugli, *Rapid Commun. Mass Spectrom.* 16 (2002) 1686.
- [16] D. Debois, A. Giuliani, O. Laprèvote, *J. Mass Spectrom.* 41 (2006) 1554.
- [17] P.J. Linstrom, W.G. Mallard (Eds.), *Nist Chemistry WebBook*, NIST Standard reference Database Number 69, June 2005. National Institut of Standards and Technology, Gaithersburg, MD, 20899 (<http://webbook.nist.gov>).
- [18] H.W. Jochims, M. Schwell, H. Baumgärtel, S. Leach, *Chem. Phys.* 314 (2005) 263.
- [19] T.J. Kauppila, R. Kostianen, A.P. Bruins, *Rapid Commun. Mass Spectrom.* 18 (2004) 808.
- [20] J. Wu, S.A. McLuckey, *Int. J. Mass Spectrom.* 237 (2004) 197.
- [21] A.K. Vrkic, R.A.J. O'Hair, S. Foote, G.E. Reid, *Int. J. Mass Spectrom.* 194 (2000) 145.
- [22] M.S. Wilson, A. McCloskey, *J. Am. Chem. Soc.* 97 (1975) 3436.
- [23] S.J. Shaw, D.M. Desiderio, K. Tsuboyama, J.A. McCloskey, *J. Am. Chem. Soc.* 92 (1970) 2510.
- [24] A. Giuliani, D. Debois, O. Laprèvote, *Eur. J. Mass Spectrom.* 12 (2006) 189.
- [25] A.M. Kamel, B. Munson, *Eur. J. Mass Spectrom.* 10 (2004) 239.